NUMERICAL SIMULATION OF PARTIAL SLIP CONTACT USING A SEMI-ANALYTICAL METHOD

J. Armand
Imperial College London
London, UK

L. Salles
Imperial College London
London, UK

C. W. Schwingshackl
Imperial College London
London, UK

ABSTRACT

Almost all mechanical structures consist of an assembly of components that are linked together with joints. If such a structure experiences vibration during operation, micro-sliding can occur in the joint, resulting in fretting wear. Fretting wear affects the mechanical properties of the joints over their lifetime and as a result impacts the non-linear dynamic response of the system. For accurate prediction of the non-linear dynamic response over the lifetime of the structure, fretting wear should be considered in the analysis.

Fretting wear studies require an accurate assessment of the stresses and strains in the contacting surfaces of the joints. To provide this information, a contact solver based on the semi-analytical method has been implemented in this study. By solving the normal and tangential contact problems between two elastic semi-infinite bodies, the contact solver allows an accurate calculation of the pressure and shear distributions as well as the relative slips in the contact area. The computed results for a smooth spherical contact between similar elastic materials are presented and validated against analytical solutions. The results are also compared with those obtained from finite element simulations to demonstrate the accuracy and computational benefits of the semi-analytical method. Its capabilities are further illustrated in a new test case of a cylinder with rounded edges on a flat surface, which is a more realistic contact representation of an industrial joint.

INTRODUCTION

A mechanical joint submitted to vibrations may be prone to micro-slidings; these are likely to produce fretting wear that can significantly affect the mechanical properties of the joint and consequently its non-linear dynamic behaviour [1, 2]. To study fretting wear and its impact on dynamic behaviour, an assessment of the stress and strain in the contacting surfaces of the joint is required. Three common tools are available to obtain these contact parameters: analytical solutions, semi-analytical approaches and the Finite Element Method (FEM).

Analytical solutions, based on complex mathematical models, are available for only a few elementary problems. Hertz [3] first introduced an analytical solution for normal contact of elastic bodies and considered the contact of smooth and non-conforming surfaces. The Hertzian theory is based on the following assumptions: the contact area is elliptical, the contact is frictionless and the elastic half-space body description is used. The last assumption is only valid when the contact area is small compared to the dimensions of the contacting bodies, which ensures that stresses are concentrated close to the contact area and are not influenced by distant boundary conditions. Analytical solutions for frictional contact have also been introduced and most assume a uniform Coulomb friction coefficient. The solutions are given by McEwen [4] for cylindrical contact, Sackfield and Hills [5] for elliptical contact and Hamilton and Goodman [6] for spherical contact. Another important spherical contact problem, solved by Cattaneo [7] and Mindlin [8], is the spherical contact subjected to stick-slip behaviour, showing that even when the contacting bodies are almost under full stick condition, a periph-

eral slipping annulus appears. This behaviour is within the theory of elasticity and obeys the Coulomb friction law. Lubkin [9] extended the above approach by formulating the solution for the torsion of elastic spheres in contact.

Most of these analytical solutions are only applicable to two-dimensional problems and the few existing three-dimensional solutions assume a symmetry of revolution, which makes it very difficult to use them for engineering problems, hence the use of numerical methods to find accurate stress and strain distributions in the contact area. The FEM has been widely used in contact mechanics [10, 11, 12, 13, 14]. However, mesh convergence [15] requires an extremely fine mesh to solve contact analysis with the FEM, which leads to long set-up times, convergence issues and large computational cost.

To overcome the limitations of both FEM and analytical solutions, an alternative tool called the Semi-Analytical Method (SAM) has recently been developed [16, 17, 18, 19]. It consists of a numerical summation of elementary solutions in a contact solver scheme. In this approach, only a small region enclosing the contact area is meshed, which leads to a dramatic reduction in the computational time compared to FEM. Bentall and Johnson [20] and Paul and Hashemi [21] were the first to introduce this method, after which Kalker [22] presented a mathematical formulation of SAM and proposed an algorithm for its resolution. One of the advantages of SAM is that acceleration techniques such as the Multigrid method [23, 24] and the fast Fourier transforms method [25, 26, 27] can be used to further reduce computational time. To extend the range of application of SAM, Chen and Wang [16] presented a three-dimensional numerical model for the simulation of non-conforming contacts of dissimilar elastic materials. Following this work, Wang et al. [17] investigated the additional effect of a torsional moment. Using an incremental approach, Gallego et al. [18] developed an algorithm to study different fretting modes and found that assumptions adopted in the analytical solutions lead to inaccurate results; they later demonstrated the benefits of using SAM within a multi-scale approach for fretting wear analysis [28]. Spinu and Amarandei [19] also used an incremental iterative algorithm for the fully coupled elastic contact with slip and stick behaviour.

In the present study, an implementation of SAM is validated against analytical solutions for the elastic spherical contact and the results are compared with FEM simulations. Its capabilities are further illustrated in a new test case consisting of a cylinder with rounded edges on a flat surface, which is a more realistic contact representation for industrial joints. This extends the work of Goryacheva et al. [29] on the two-dimensional partial slip contact of an inclined punch with rounded edges.

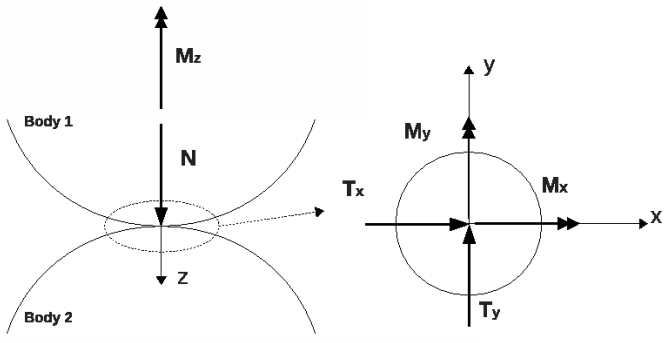

FIGURE 1: CONTACT BETWEEN TWO SIMILAR ELASTIC SEMI-INFINITE BODIES

THE SEMI-ANALYTICAL CONTACT SOLVER

Following the works of Gallego et al. [18] and Spinu and Amarandei [19], a contact solver using the Semi-Analytical Method was implemented to solve the quasi-static contact equilibrium, i.e. the normal and the tangential contact problems. This contact solver is based on the use of the projected conjugate gradient method [27] and a discrete-convolution fast Fourier transform to accelerate the computation. The approach assumes the elastic half-space body description, which makes it possible to use the Boussinesq and Cerruti potentials [30, 31] to compute the elastic deflections in the normal and tangential directions from the pressures and shear tractions in the contact area. In the case of the contact of similar elastic materials, it is known that no coupling exists between the normal and the tangential problem. In other words, the normal displacements are independent of the shear tractions and tangential displacements are independent of the pressure. However, a coupling between the two tangential directions exists even for similar elastic materials.

In the following, the main components of the numerical algorithm used in this study are introduced; for more details please refer to the literature. Figure 1 illustrates the contact between two similar elastic semi-infinite bodies. A normal load N, tangential forces T_x and T_y, bending moments M_x and M_y and a twisting moment M_z are consecutively applied to the upper body 1 while the lower body 2 is fixed. The values of the loads are selected to produce a partial slip condition.

The first step of the algorithm is to solve the normal contact problem, which is done by finding a pressure distribution p that gives a closed gap $g = 0$ in the contact area and an open gap $g \geq 0$ outside the contact area:

$$\begin{aligned} p \geq 0,\ g = u_z + h - \delta_z - y\phi_x + x\phi_y = 0 \\ p = 0,\ g = u_z + h - \delta_z - y\phi_x + x\phi_y \geq 0 \end{aligned} \tag{1}$$

where u_z is the surface elastic deformations in the z direction, h is the initial normal separation between the two contacting surfaces,

δ_z is the rigid body displacement of the surfaces in the vertical direction, and $y\phi_x$ and $x\phi_y$ are the displacements resulting from small rigid body rotations ϕ_x and ϕ_y.

The computed pressure distribution must also fulfil the following force and moment equilibrium equations:

$$\begin{array}{c} \iint p(x,y)\, dxdy = N, \\ \iint\ y\ p(x,y)\, dxdy = -M_x, \\ \iint x\ p(x,y)\, dxdy = M_y \end{array} \tag{2}$$

Such a pressure distribution can be found using the conjugate gradient method (CGM) algorithm with Eq. 1 and Eq. 2 as constraint conditions. The reader may refer to [18, 19] for more details.

Once the normal problem is solved, the shear q_x, q_y and the slip s_x, s_y can be found. They must obey the Coulomb friction law, leading to the following constraint equations:

$$\begin{array}{l} \sqrt{q_x^2+q_y^2} \le \mu p, \ \ \sqrt{s_x^2+s_y^2} = 0, \ \ (x,y) \in A_{st} \\ \sqrt{q_x^2+q_y^2} = \mu p, \ \ \sqrt{s_x^2+s_y^2} \ge 0, \ \ (x,y) \in A_{sl} \end{array} \tag{3}$$

where A_{st} denotes the stick element set and A_{sl} the slip element set. s_x and s_y are given by:

$$\begin{bmatrix} s_x \\ s_y \end{bmatrix} = \begin{bmatrix} u_x \\ u_y \end{bmatrix} - \begin{bmatrix} \delta_x + y\phi_z \\ \delta_y - x\phi_z \end{bmatrix} \tag{4}$$

In the semi-analytical method, the elastic surface deformations u_x, u_y and u_z are calculated using the influence coefficients $C_{p,q}^{ij}$ that can be found in [17]:

$$\begin{bmatrix} u_x \\ u_y \\ u_z \end{bmatrix} = \begin{bmatrix} u_{xx}+u_{xy}+u_{xz} \\ u_{yx}+u_{yy}+u_{yz} \\ u_{zx}+u_{zy}+u_{zz} \end{bmatrix} = \begin{bmatrix} C_{q_x}^{xx} & C_{q_y}^{xy} & C_p^{xz} \\ C_{q_x}^{yx} & C_{q_y}^{yy} & C_p^{yz} \\ C_{q_x}^{zx} & C_{q_y}^{zy} & C_p^{zz} \end{bmatrix} \begin{bmatrix} q_x \\ q_y \\ p \end{bmatrix} \tag{5}$$

The equilibrium in terms of tangential loads is given by:

$$\begin{array}{c} \iint q_x(x,y)\, dxdy = T_x, \\ \iint\ q_y(x,y)\, dxdy = T_y, \\ \iint (xq_y(x,y) - yq_x(x,y))\, dxdy = M_z \end{array} \tag{6}$$

The shear tractions q_x and q_y can be determined in a similar way to the pressure distribution by using the CGM algorithm with the constraint conditions given by Eq. 3 and Eq. 6. The details are provided by Gallego et al. in [18]. The whole numerical procedure is summarized in a flow chart (Fig. 2). The implemented contact solver has been developed to be used within a multi-scale approach for fretting wear studies. In this approach, proposed by Gallego [28], the input loads of the contact solver (N, T_x, T_y, M_x, M_y, M_z) are extracted in the contact area from a non-linear dynamic analysis. The semi-analytical method allows a much finer discretisation of the contact area than that used for dynamic calculations, and as a result provides a more accurate pressure, shear and slip distributions for wear computation.

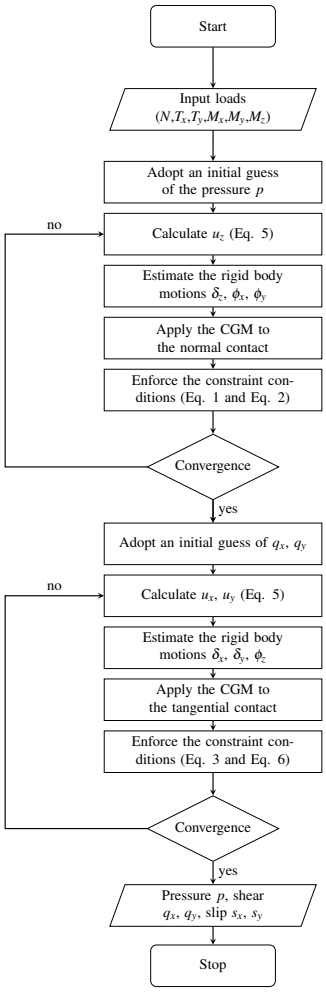

FIGURE 2: FLOW CHART OF THE CONTACT ALGORITHM

VALIDATION OF SAM

Model

The validation of the implementation and the capabilities of SAM was performed on the smooth spherical contact (see Fig. 3), for which an analytical solution is available. The spheres are pressed together with a normal load N, and depending on the case under consideration, a tangential load T or a twisting moment M_z is also applied, both of which are chosen to produce

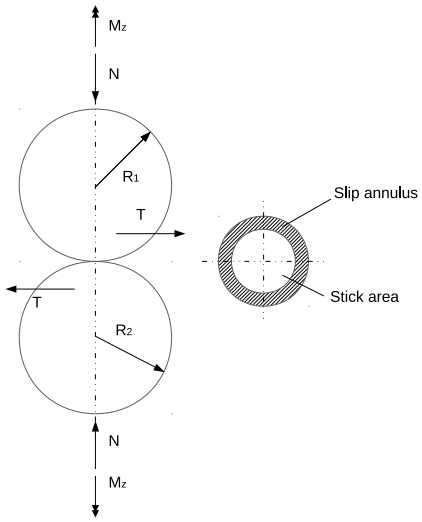

FIGURE 3: SMOOTH CONTACT BETWEEN TWO SPHERES

partial slip conditions. All calculation parameters are given in Tab. 1 . The results were obtained on a regular grid of 512×512 elements with $-1.5a < x < 1.5a$ and $-1.5a < y < 1.5a$.

TABLE 1: CALCULATION PARAMETERS

Parameter	Value
Young's modulus of sphere 1, E_1 (GPa)	210
Young's modulus of sphere 2, E_2 (GPa)	210
Poisson ratio of sphere 1, ν_1	0.3
Poisson ratio of sphere 2, ν_2	0.3
Friction coefficient, μ	0.1
Radius of sphere 1, R_1 (m)	0.2
Radius of sphere 2, R_2 (m)	0.2
Normal load, N (N)	1,000
Tangential load, T_x (N)	[0 - 1] * μN
Limit twisting moment, M_{lim} (N.mm)	51.0257
Twisting moment, M_z (N.mm)	[0 - 1] * M_{lim}
Maximum Hertzian pressure, p_o (MPa)	636.3057
Hertzian contact radius, a (mm)	0.8662

Results

The results are normalised by the maximum Hertzian pressure p_o and the Hertzian contact radius a. Figure 4 compares the pressure distribution p obtained with SAM to the Hertzian theory [3] for a centrally applied normal load. The good agreement between the calculated pressure distribution and the analytical solution validates the implementation of the normal part of the contact solver.

As a first validation of the tangential part of the contact solver, the computed shear and slip distributions under a tangential load T_x have been compared with the Cattaneo-Mindlin results [7, 8]. Figures 5 and 6 display respectively the shear and the slip distributions for different values of the dimensionless tangential load $\bar{T}_x = \frac{T_x}{\mu N}$. The present results also show a good agreement with the analytical solution.

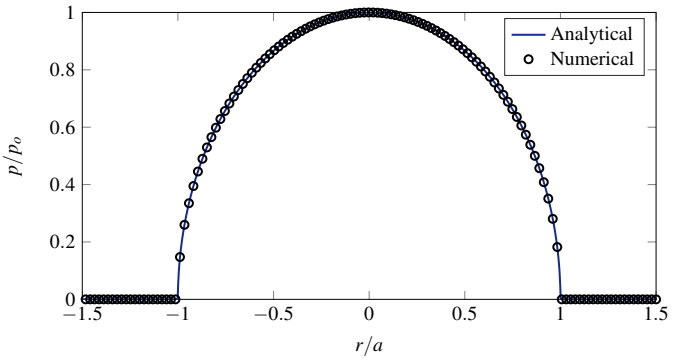

FIGURE 4: SAM PRESSURE DISTRIBUTION (NUMERICAL) AGAINST THE HERTZIAN THEORY (ANALYTICAL)

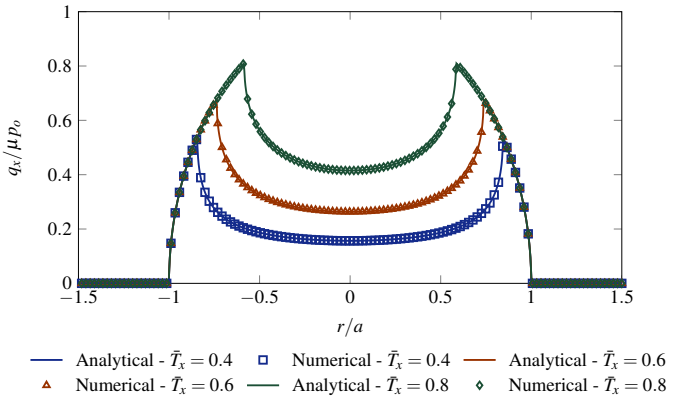

FIGURE 5: SAM SHEAR DISTRIBUTION (NUMERICAL) AGAINST CATTANEO-MINDLIN THEORY (ANALYTICAL)

To complete the validation of the tangential part of the contact solver, its results under a twisting moment have been compared with Lubkin's solution [9]. These results are presented in Fig. 7 and validate the coupling between the two tangential directions.

These results indicate that the implementation of SAM was successful. In the next section, SAM is compared with classic FE analysis to highlight its computational benefits.

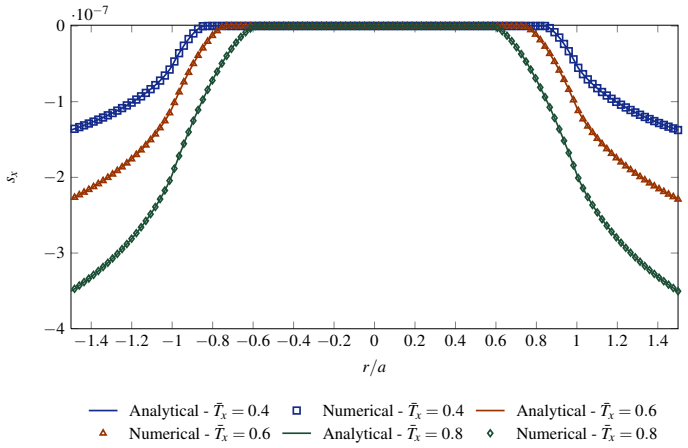

FIGURE 6: SAM SLIP DISTRIBUTION (NUMERICAL) AGAINST CATTANEO-MINDLIN THEORY (ANALYTICAL)

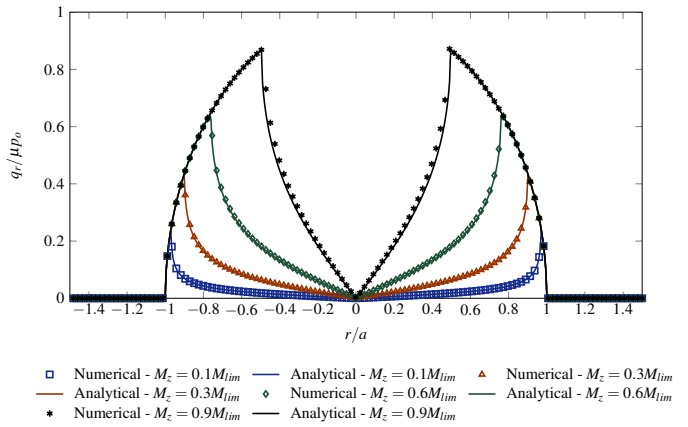

FIGURE 7: SAM SHEAR DISTRIBUTION (NUMERICAL) AGAINST LUBKIN'S THEORY (ANALYTICAL)

FINITE ELEMENT ANALYSIS

Model

To demonstrate the computational benefits of SAM, the spherical contact described in Fig. 3 was modelled with the finite element software Abaqus. The mesh depicted in Fig. 8, identical for both spheres, is composed of approximately 83,000 8-node hex elements and 88,000 nodes. The mesh size is particularly small in the region enclosing the contact area, where the radial spacing of the elements is approximately 1 mm (the hemisphere radius is 200 mm) and each element spans 7.5 deg circumferentially, leading to approximately 2,500 elements. To avoid convergence issues inherent to the non-conforming nature of this contact, the simulation is displacement-controlled (SAM can be either load-controlled or displacement-controlled, which makes the comparison with FE results possible). A vertical displacement is applied on the top surface of one sphere, while the bottom surface of the other is fixed. The material properties are the same as those given in Tab. 1. The Augmented Lagrange approach is used to solve the normal contact problem in Abaqus.

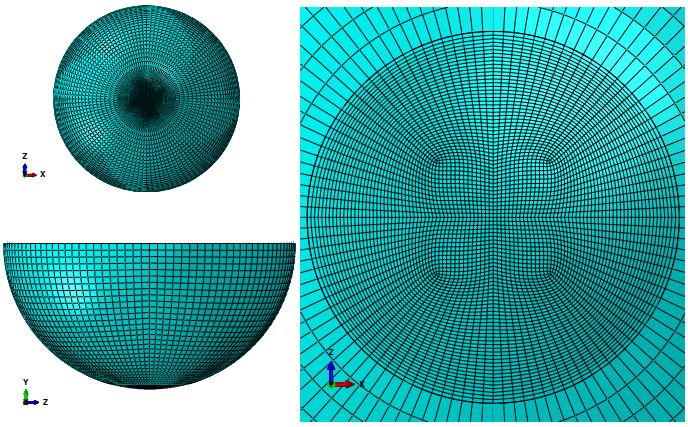

FIGURE 8: FINITE ELEMENT MESH OF SPHERE 1

Results

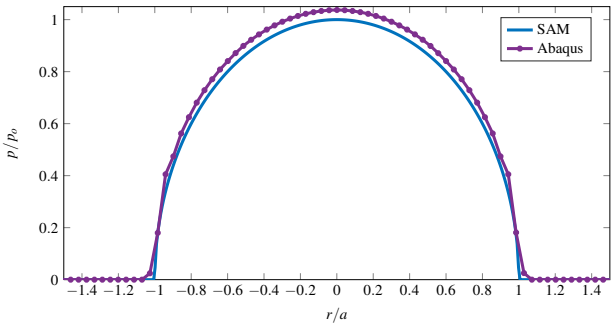

FIGURE 9: SAM PRESSURE DISTRIBUTION COMPARED TO FE RESULTS

As illustrated in Fig. 9, the FEM results show a quite good agreement with SAM and hence with the Hertzian theory. The differences can be explained by the elastic half-space assumption used by Hertz and within the semi-analytical method: when the elastic half-space assumption is verified, i.e. when the dimensions of the contact area can be considered small compared to the dimensions of the contacting bodies, the analytical solution is the most accurate. If this assumption does not hold, the converged FEM solution is assumed to give the best estimation. The key difference between FEM and SAM is the computational speed. Even with a higher number of elements used in SAM (more than 260,000 elements compared to 83,000 for FEM), computation

was much faster, as demonstrated in Tab. 2. Furthermore, it should be noted that the time given in Tab. 2 only considers the measurable computation time, and ignores the time required to set up the FE analysis. This proves the computational benefits of the semi-analytical method.

TABLE 2: FEM COMPUTATIONAL SPEED COMPARED TO SAM

	Abaqus	SAM
Memory usage	8.1 GB	689 MB
CPU time (s)	1385	4.83
Number of core	1	1

APPLICATION TO THE CONTACT BETWEEN A CYLINDER WITH ROUNDED EDGES AND A FLAT SURFACE

To further illustrate the capabilities of the contact solver, it has been applied to the contact between a cylinder with rounded edges and a flat surface, which is a more realistic representation of an industrial joint. The previously introduced six loading cases were applied to this test case.

Model

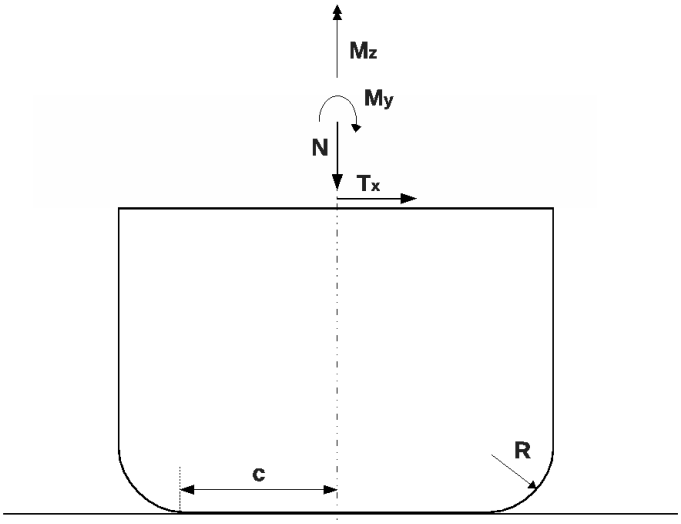

FIGURE 10: SMOOTH CONTACT BETWEEN A CYLINDER WITH ROUNDED EDGES AND A FLAT SURFACE

Figure 10 illustrates the contact of an elastic cylinder having a flat base with rounded edges with an elastic half-plane. The flat part of the cylinder base is of length $2c$ and R is the radius of curvature of the rounded edges. The cylinder is submitted to a normal load N, tangential load T_x along the x direction, bending moment M_y around the y direction and a twisting moment M_z. The model set-up parameters are given in Tab. 3. The grid consists of 512×512 elements with $-1.5c < x < 1.5c$ and $-1.5c < y < 1.5c$. The plotted results are the dimensionless pressure $\bar{p} = \frac{2pR}{E^* c}$ and shear $\bar{q} = \frac{2qR}{\mu E^* c}$, where p and q are the computed pressure and shear distributions, and $\frac{1}{E^*} = \frac{1-\nu_1^2}{E_1} + \frac{1-\nu_2^2}{E_2}$.

TABLE 3: CALCULATION PARAMETERS

Parameter	Value
Young's modulus of the cylinder, E_1 (GPa)	210
Young's modulus of the half-plane, E_2 (GPa)	210
Poisson ratio of the cylinder, ν_1	0.3
Poisson ratio of the half-plane, ν_2	0.3
Friction coefficient, μ	0.1
Radius of rounded edges, R (m)	0.2
Radius of the flat cylinder base, c (m)	0.02
Normal load, N (N)	1e6
Tangential load, T_x (N)	[0 - 1] * μN
Bending moment, M_y (N.m)	[0 - 3] * 1e4
Twisting moment, M_z (N.m)	[0 - 2] * 1e3

Results

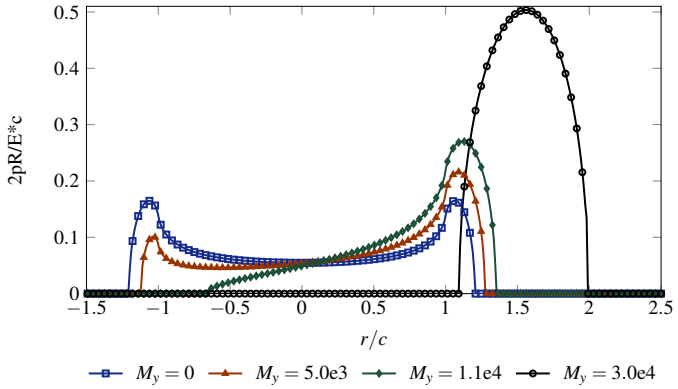

FIGURE 11: PRESSURE DISTRIBUTION UNDER VARYING BENDING MOMENT M_y

The first results presented in Fig. 11 were obtained under a normal load N combined with a bending moment around the y direction M_y. The application of the moment M_y leads to an asymmetry of the pressure distribution with respect to the axis of symmetry of the cylinder. As this moment increases, the contact area reduces and the maximum contact pressure consequently increases. The contact area moves towards one end of the cylinder

base depending on the sign of the applied bending moment. For a large value of the bending moment, only one local maximum pressure is obtained at the rounded edges when the contact area tends to zero and the contact becomes a Hertzian contact.

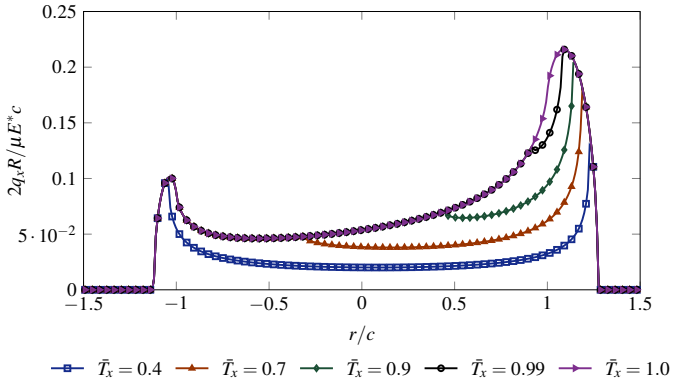

FIGURE 12: SHEAR DISTRIBUTION UNDER VARYING TANGENTIAL LOAD

The shear distribution q_x obtained for different values of the dimensionless tangential load $\bar{T}_x = \frac{T_x}{\mu p}$ combined with a constant bending moment $M_y = 5\text{e}3\ N.m$ is shown in Fig. 12. As expected, the slip area increases with the tangential load. The shear distribution is no longer symmetric with respect to the axis of symmetry of the cylinder and when increasing the tangential load, the stick zone shrinks and moves towards one end of the cylinder base.

The SAM results on these first two loading cases are consistent with those obtained by Goryacheva et al. for the 2D partial slip contact of an inclined punch with rounded edges [29], but the advantage of a full 3D SAM model is its additional capability to take into account the coupling between the tangential directions.

The results presented in Fig. 13 are obtained under a constant normal load N combined with a varying twisting moment M_z. Under these symmetric loads, the shear distribution q_r (equal to $\sqrt{q_x^2+q_y^2}$) remains symmetric with respect to the axis of symmetry of the cylinder. The results are comparable to those obtained for the torsional spherical contact described by Lubkin [9]. As the twisting moment increases, the slip annulus progresses inward and eventually shrinks to the centre of the contact area (gross slip).

This test case highlights the flexibility of SAM in terms of contact geometry that can be simulated. Unlike the analytical solutions, SAM can be easily applied to a geometry representative of an industrial application. Furthermore, this test case proves that SAM can handle all possible loads (normal, tangential, bending and twisting moments) which makes it readily usable in a multi-scale approach for fretting wear studies.

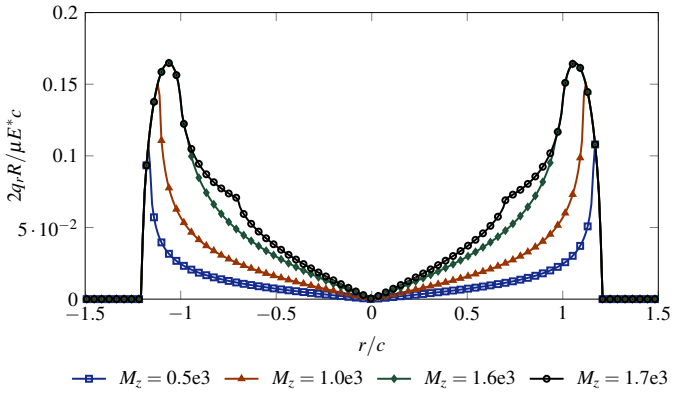

FIGURE 13: SHEAR DISTRIBUTION FOR DIFFERENT VALUES OF TWISTING MOMENT M_z

However, the half-space assumption places geometrical restrictions on the contact since the dimensions of the contact area must be small compared to the dimensions of the contacting bodies, which may restrict the use of the semi-analytical method in industrial applications.

CONCLUSIONS

The Semi-Analytical Method (SAM) has been shown to be a powerful tool to solve a partial slip contact problem. The accuracy of the semi-analytical method was demonstrated by comparisons with analytical solutions for the spherical contact between similar elastic semi-infinite bodies, and the computational benefits of this approach were illustrated by comparing it with FE analysis. The capabilities of SAM were further illustrated by the test case of a cylinder with rounded edges in contact with an elastic half-plane. The semi-analytical method provides an accurate and fast approach to evaluate the stresses and strains in the contact area, which makes it a powerful tool for future fretting wear studies and an investigation of the impact of fretting wear on the non-linear dynamic response over the lifetime of a component.

ACKNOWLEDGMENT

The authors are grateful to Innovate UK and Rolls-Royce Plc. for providing the financial support for this work and for giving permission to publish it. Special thanks go to Dr. D. Dini from Imperial College London for his useful comments on SAM.

REFERENCES

[1] Schwingshackl, C. W., Petrov, E. P., and Ewins, D. J., 2012. “Effects of Contact Interface Parameters on Vibration

of Turbine Bladed Disks With Underplatform Dampers". *Journal of Engineering for Gas Turbines and Power,* ***134***(3), p. 032507.

[2] Salles, L., Blanc, L., Thouverez, F., and a.M. Gouskov, 2011. "Dynamic analysis of fretting-wear in friction contact interfaces". *International Journal of Solids and Structures,* ***48***(10), May, pp. 1513–1524.

[3] Hertz, H., 1881. "On the contact of elastic solids". *J. reine angew. Math,* ***92***(156-171), p. 110.

[4] M'Ewen, E., 1949. "Xli. stresses in elastic cylinders in contact along a generatrix (including the effect of tangential friction)". *Philosophical Magazine,* ***40***(303), pp. 454–459.

[5] Sackfield, A., and Hills, D., 1983. "Some useful results in the classical hertz contact problem". *The Journal of Strain Analysis for Engineering Design,* ***18***(2), pp. 101–105.

[6] Hamilton, G., and Goodman, L., 1966. "The stress field created by a circular sliding contact". *Journal of Applied Mechanics,* ***33***(2), pp. 371–376.

[7] Cattaneo, C., 1938. "Sul contatto di due corpi elastici: distribuzione locale degli sforzi". *Rendiconti dell'Aecademia Nazionale dei Lincei,* ***27***, pp. 342–348,434–436,474–478.

[8] Mindlin, R., 1949. "Compliance of elastic bodies in contact". *Trans.ASME, Series E, Journal of Applied Mechanics,* ***16***, pp. 259–268.

[9] Lubkin, J. L., 1951. "The torsion of elastic spheres in contact". *Journal of Applied Mechanics-Transactions of the ASME,* ***18***(2), pp. 183–187.

[10] Komvopoulos, K., and Choi, D.-H., 1992. "Elastic finite element analysis of multi-asperity contacts". *Journal of tribology,* ***114***(4), pp. 823–831.

[11] Kral, E., Komvopoulos, K., and Bogy, D., 1993. "Elastic-plastic finite element analysis of repeated indentation of a half-space by a rigid sphere". *Journal of applied mechanics,* ***60***(4), pp. 829–841.

[12] Kucharski, S., Klimczak, T., Polijaniuk, A., and Kaczmarek, J., 1994. "Finite-elements model for the contact of rough surfaces". *Wear,* ***177***(1), pp. 1–13.

[13] Kogut, L., and Etsion, I., 2002. "Elastic-plastic contact analysis of a sphere and a rigid flat". *Journal of Applied Mechanics,* ***69***(5), pp. 657–662.

[14] Durand, J., Yastrebov, V., Proudhon, H., Cailletaud, G., et al., 2011. "Finite element analysis of the contact between rough surfaces". In Advances in Heterogeneous Material Mechanics 2011: Proceedings of the Third International Conference on Heterogeneous Material Mechanics: May 22-26, 2011, Shanghai, China, Vol. 13, DEStech Publications, Inc, p. 47.

[15] Reddy, J. N., 1993. *An introduction to the finite element method*, Vol. 2. McGraw-Hill New York.

[16] Chen, W. W., and Wang, Q. J., 2008. "A numerical model for the point contact of dissimilar materials considering tangential tractions". *Mechanics of Materials,* ***40***(11), pp. 936 – 948.

[17] Wang, Z., Meng, F., Xiao, K., Wang, J., and Wang, W., 2011. "Numerical analysis of partial slip contact under a tangential force and a twisting moment". *Proceedings of the Institution of Mechanical Engineers, Part J: Journal of Engineering Tribology,* ***225***(2), pp. 72–83.

[18] Gallego, L., Nélias, D., and Deyber, S., 2010. "A fast and efficient contact algorithm for fretting problems applied to fretting modes I, II and III". *Wear,* ***268***(1-2), Jan., pp. 208–222.

[19] Spinu, S., and Amarandei, D., 2012. "Numerical simulation of slip-stick elastic contact.".

[20] Bentall, R., and Johnson, K., 1967. "Slip in the rolling contact of two dissimilar elastic rollers". *International journal of mechanical sciences,* ***9***(6), pp. 389–404.

[21] Paul, B., and Hashemi, J., 1981. "Contact pressures on closely conforming elastic bodies". *Journal of Applied Mechanics,* ***48***(3), pp. 543–548.

[22] Kalker, J. J., 1990. *Three-dimensional elastic bodies in rolling contact*, Vol. 2. Springer.

[23] Brandt, A., and Lubrecht, A., 1990. "Multilevel matrix multiplication and fast solution of integral equations". *Journal of Computational Physics,* ***90***(2), pp. 348–370.

[24] Lubrecht, A., and Ioannides, E., 1991. "A fast solution of the dry contact problem and the associated sub-surface stress field, using multilevel techniques". *Journal of tribology,* ***113***(1), pp. 128–133.

[25] Ju, Y., and Farris, T., 1996. "Spectral analysis of two-dimensional contact problems". *Journal of tribology,* ***118***(2), pp. 320–328.

[26] Liu, S., Wang, Q., and Liu, G., 2000. "A versatile method of discrete convolution and fft (dc-fft) for contact analyses". *Wear,* ***243***(1), pp. 101–111.

[27] Polonsky, I., and Keer, L., 2000. "Fast methods for solving rough contact problems: a comparative study". *Journal of tribology,* ***122***(1), pp. 36–41.

[28] Gallego, L., Fulleringer, B., Deyber, S., and Nélias, D., 2010. "Multiscale computation of fretting wear at the blade/disk interface". *Tribology International,* ***43***(4), pp. 708–718.

[29] Goryacheva, I., 2002. "Contact problem with partial slip for the inclined punch with rounded edges". *International Journal of Fatigue,* ***24***(11), Nov., pp. 1191–1201.

[30] Johnson, K. L., 1985. *Contact Mechanics*. Cambridge University Press. Cambridge Books Online.

[31] Love, A., 1906. *A Treatise on the Mathematical Theory of Elasticity*. A Treatise on the Mathematical Theory of Elasticity. at the University Press.